Scientific Reports

https://doi.org/10.1038/s41598-026-62407-4

Article in Press

Juvenile hormone signaling acts during development and post-mating to suppress antibacterial defenses in *Drosophila melanogaster*

Received: 20 February 2026

Accepted: 10 July 2026

Published online: 16 July 2026

Cite this article as: Keith S.A., Gupta V., Kalukin A.A. *et al.* Juvenile hormone signaling acts during development and post-mating to suppress antibacterial defenses in *Drosophila melanogaster*. *Sci Rep* (2026). https://doi.org/10.1038/s41598-026-62407-4

Scott A. Keith, Vanika Gupta, Ananda A. Kalukin & Brian P. Lazzaro

Juvenile hormone signaling acts during development and post-mating to suppress antibacterial defenses in *Drosophila melanogaster*

Scott A. Keith[1,2], Vanika Gupta[1,2,3], Ananda A. Kalukin[1,2], Brian P. Lazzaro[1,2]

1. Department of Entomology, College of Agriculture and Life Sciences, Cornell University, Ithaca, NY, 14853, United States of America
2. Cornell Institute of Host-Microbe Interactions & Disease, Cornell University, Ithaca, NY, 14853, United States of America
3. Department of Zoology, University of Delhi, Delhi – 110007, India

Corresponding author:

Scott A. Keith

Email: sk2649@cornell.edu

Keywords: Juvenile hormone, *Drosophila melanogaster*, bacterial infection, reproduction, metamorphosis, adipocytes

ABSTRACT

Reproductive investment is frequently associated with compromised immune performance. In female *Drosophila melanogaster*, mating increases susceptibility to bacterial infections, and prior work has demonstrated that juvenile hormone (JH) signaling is necessary for this mating-induced reduction of immune performance. However, the temporal dynamics and key organ systems that mediate this JH-mediated immunosuppression have not been studied. Here we show that post-mating sensitivity to bacterial infection depends on JH function spanning multiple life stages and target tissues. We find that mating induces a rapid, transient peak in JH titers and prolonged JH signaling activity. Transient treatment with exogenous JH is not sufficient to increase mortality from infection, suggesting continued JH activity is necessary for the persistent immune suppression observed after mating. Using conditional RNAi, we find that the JH receptor germ cells expressed (Gce) functions in the adipose tissue of developing pupae

to potentiate post-mating sensitivity to infection in adults. In adult females, Gce appears to function in multiple tissues, including the fat body and ovary, to decrease infection resistance after mating. These results suggest that Gce function during metamorphic development sensitizes adult females to sustained JH signaling induced by mating. More broadly, our study illustrates how endocrine regulation of the interaction between development and reproduction can shape immune performance and infection outcome.

INTRODUCTION

Animal immune systems are profoundly influenced by direct and indirect integration with other physiological processes. Reproductive investment constrains and antagonizes immune performance across a variety of vertebrate and invertebrate taxa[1–3]. In *Drosophila melanogaster*, mated, reproducing females experience substantially increased mortality when orally or systemically infected with a variety of bacterial pathogens[4–16]. Mating-induced immune suppression occurs rapidly, with females showing increased sensitivity to bacterial infection as quickly as 2.5 hours after mating[5], and persists for at least ten days following mating[7]. Thus, a single mating is sufficient to trigger lasting inhibition of immune defenses in female *D. melanogaster*.

Mating stimulates dynamic endocrine networks that promote reproduction[17], including activation of juvenile hormone (JH) signaling[18–20]. JH also regulates insect immunity[21–28], and in *D. melanogaster* primarily acts as an immunosuppressant[9,14,29]. Prior work has shown that JH signaling is required for mating-induced immune suppression in female *D. melanogaster*[9]. However, almost nothing is known about the signaling dynamics or mechanistic factors downstream of mating-activated JH production that ultimately reduce the ability of mated females to withstand infection.

Juvenile hormones constitute a group of chemically-related sesquiterpenoid hormones that regulate many aspects of insect physiology[30–33]. Among these functions, JH has been most thoroughly studied for its role in controlling larval development and metamorphosis[34]. JH also sustains reproductive activity and oogenesis in adult females[17,35], including by stimulating the production of yolk proteins (or "vitellogenins") that are deposited into the oocyte[36–39]. In larvae and adults, JH molecules are synthesized by an endocrine gland called the corpus allatum[40]. Secreted JH circulates through the hemolymph and binds JH receptors, which function as basic Helix-Loop-Helix/Per-ARNT-SIM transcription factors to regulate gene expression and transduce JH-activated cellular and physiological processes[41].

Drosophilids possess two paralogous JH receptors, encoded by the genes *Methoprene tolerant* (*Met*, an evolutionarily derived duplication) and *germ cells expressed* (*gce*, the more ancestral receptor)[42–46]. Schwenke & Lazzaro (2017) used a tissue-ubiquitous RNA interference (RNAi) approach to demonstrate that Gce is required for post-mating immune suppression. However, the specific organs or cell types in which Gce acts to reduce immune defenses in mated females have not been determined. Furthermore, in that study, genetic disruption of *gce* expression was induced at the onset of metamorphosis and maintained throughout early adulthood. Given the critical roles of JH activity in coordinating both development and reproduction, it remains unclear whether Gce curtails immunity entirely through post-mating JH signaling, or whether metamorphic functions of Gce might also be involved.

Here we show that mating induces sustained JH signaling activity, corresponding to the sustained immune suppression experienced by mated females, and that continual

presence of the hormone is necessary to induce sensitivity to bacterial infection. Additionally, we find that Gce activity in multiple tissues of pupae and adult female *D. melanogaster* reduces post-mating resistance to infection.

RESULTS

Juvenile Hormone treatment reduces immune defenses of virgin females

The JH analog methoprene has been shown to attenuate immune gene expression[9,29] and infection resistance[9] in virgin female *D. melanogaster*. However, methoprene is more stable and potent than endogenous JH[44,47], so the measured effects of methoprene treatment could be artificially strong. For the present study, we performed a dose-response assay to test whether exogenous JH III would be sufficient to increase infection susceptibility of unmated females, thus chemically mimicking the immune-suppressive effects of mating. We exposed Canton-S virgin females to filter discs infused with 0.005 µg to 2 µg of JH III dissolved in acetone and assayed survival following infection with the bacterial pathogen *Providencia rettgeri*[48]. Females were exposed to the volatilized hormone for 24 hours to allow passive uptake (see Materials & Methods), then were infected with *P. rettgeri*, placed in fresh JH vials, and monitored for survival. Infected flies were transferred to fresh JH vials daily throughout the five days over which we recorded survival. To establish a baseline prediction for the expected decrease in resistance to infection, we challenged *D. melanogaster* females with *P. rettgeri* at either 6 hours or 4 days after mating and measured survival for five days post-infection. Consistent with prior studies[5–8,10,11,13,15,16], mated females experienced significantly higher infection-induced mortality than virgin females when challenged at either of these post-mating timepoints (Fig. 1A, B).

We found that ectopic exposure to 0.005 µg, 0.05 µg, or 0.5 µg of JH III had no effect on infection susceptibility. Females housed in vials with these doses survived *P. rettgeri* infection comparably to control females housed in vials containing filter paper saturated with an equivalent volume of acetone vehicle (Fig. 1C). In contrast, virgin females exposed to 1 µg or 2 µg of JH III were significantly more sensitive to *P. rettgeri* infection than vehicle-exposed control females, and were more susceptible than females exposed to the three lower concentrations (Fig. 1C). The mortality of infected unmated females exposed to 1 µg or 2 µg of JH III was quantitatively similar to that of mated females, whereas the survival of unmated females exposed to lower JH III doses was similar to that of unmated females (compare Fig. 1C to Fig. 1A and Fig. 1B). Importantly, ≥96% of flies exposed to the high JH doses survived injury with a needle dipped in sterile PBS (n=26 for 1 µg JH III and n=21 for 2 µg JH III), indicating that the mortality of *P. rettgeri*-challenged females was not due to toxicity of the hormone exposure or a consequence of injury.

The reduced infection survival of unmated females exposed to 2 µg JH III suggested a biological response to the exogenous JH. To confirm this, we measured transcript levels of the known JH target genes *Kruppel homolog 1* (*Kr-h1*), *minidiscs* (*mnd*), and *Juvenile Hormone Inducible-21* (*JHI-21*)[49,50] in unmated females exposed to 2 µg JH III for 24 hours. Expression of *Kr-h1* and *mnd*, though not *JHI-21*, was significantly elevated in JH-exposed females relative to vehicle-exposed females (Fig. 1D). These data indicate that our exposure protocol and this hormone dosage are sufficient to induce JH-regulated molecular responses.

Together our results show that exposure to JH III can activate JH signaling and increase sensitivity to pathogen challenge in unmated females, thus recapitulating the reduced infection resistance caused by mating.

Mating induces a transient peak in JH titers and sustained JH signaling

The quantitative dynamics of post-mating JH activity have not been defined, allowing for two alternative mechanistic hypotheses for long-lasting immune suppression. Under the first hypothesis, a transient spike in JH activity post-mating could activate a mechanism that causes irreversible immunosuppression even in the absence of subsequent JH signaling. Under the alternative second hypothesis, JH ligand levels might remain persistently elevated following mating, leading to sustained JH signaling activity that continuously suppresses infection resistance.

To begin to differentiate these hypotheses, we profiled JH titers and JH signaling activity over time following mating. We quantified JH III levels in Canton-S females using liquid chromatography-tandem mass spectrometry (LC-MS/MS) at 2 h, 6 h, 12 h, and then every 24 h up to 4 days post-mating. To complement these measurements, we used a transgenic reporter line to measure JH signaling activity at corresponding time points. This fly line carries a transgene comprising eight tandem repeats of *JH response element* (*JHRE*) sequence[44] upstream of an *eGFP* reporter (*8xJHRE-eGFP*)[51]. As such, *GFP* expression in these flies provides an *in vivo* readout of Gce/Met-dependent JH signaling activity[51,52]. Females of this reporter strain exhibited the same rapid (Fig. S1A) and sustained (Fig. S1B) mating-induced infection susceptibility as Canton-S females (Fig. 1A, B).

We determined that JH III titers were significantly increased above virgin levels at 2 h and 6 h post-mating (Fig. 2A). Correspondingly, RT-qPCR measurement of *8xJHRE-eGFP* expression indicated that the reporter was induced ~2-fold over virgin levels at 6 h post-mating, reflecting activated JH signaling (Fig. 2B). This mating-activated *GFP* induction was not observed in flies carrying a modified construct with point-mutations in the *JHRE* sequence that prevent Gce/Met binding[44,51], demonstrating specificity and JH-receptor-dependence of the reporter signal (Fig. S1C). Notably, after the initial increase in JH III, hormone levels declined and remained consistent from 12 hours to 4 days post-mating (Fig. 2A). These titers remained modestly higher than levels in unmated females but significantly lower than peak titers at 2 h and 6 h. However, despite the decrease in JH III levels at later timepoints, *GFP* reporter expression remained consistently elevated for up to seven days post-mating (Fig. 2B). This suggests that the relatively lower levels of JH III can still elicit a robust transcriptional response several days post-mating.

Transient induction of JH signaling is not sufficient to increase infection sensitivity

Our profiling of JH dynamics indicated that either hypothesis for sustained mating-induced infection sensitivity might be possible: the early peak in JH III levels and rapid activation of JH signaling might irreversibly reduce immune defenses, or the sustained JH signaling activity over days might continuously suppress resistance to infection. We reasoned that if the first hypothesis were correct, then a single pulse of JH signaling should be sufficient to reduce infection survival. Alternatively, if the second hypothesis were correct, females that only experienced a single pulse of JH signaling would not exhibit decreased ability to withstand infection. To test this, we exposed unmated females to 2 µg JH III for 48 hours (transferring to fresh JH III once, after the first 24 hours) and

then transferred them to regular food vials for 24 hours, thus removing the hormone ligand and achieving “transient” exposure (Fig. 3A). In order to confirm that this treatment results in transient activation of JH responses, we again measured JH III levels and *8xJHRE-eGFP* expression. Six hours after initiating JH exposure we observed a modest, though not significant, increase in JH titers (Fig. 3B) and an ~2-fold induction of *8xJHRE-GFP* expression relative to vehicle-treated control flies (Fig. 3C), similar to the level of reporter induction caused by mating (Fig. 2B). Twenty-four hours after hormone removal (“72h-T”), both JH titers (Fig. 3B) and *GFP* expression levels (Fig. 3C) were indistinguishable between control flies and those that had been transiently exposed to JH.

Having validated our ability to transiently activate JH signaling, we asked whether this single induction event would be sufficient to render unmated females more susceptible to infection. We subjected Canton-S and *8xJHRE-eGFP* virgins to transient JH III exposure as described, then challenged them with *P. rettgeri* and monitored survival. In parallel, another group of unmated females was housed in vials with 2 µg JH III for the duration of the experiment, both prior to and during infection, with daily transfer to fresh exposure vials, as was done in our previous experiments (Fig. 1C). We again found that this repeated exposure significantly increased the susceptibility of both Canton-S and *8xJHRE-eGFP* virgins to *P. rettgeri* (Fig. 3). In contrast, the post-infection survival of transiently-exposed females that were infected 24 hours after hormone removal was comparable to that of control females exposed to the acetone vehicle (Fig. 3D, E). Thus, a single period of JH signal induction with no further hormone stimulus prior to or during infection is not sufficient to recapitulate the weakened immune performance induced by mating or repeated JH III exposure. This result does not support the hypothesis of a

transient initial burst of JH activity that triggers lasting, diminished infection resistance. Rather, our findings suggest that continuously active JH signaling is necessary for post-mating reduction in the ability of female flies to survive infection.

Mating-induced infection susceptibility requires the JH receptor Gce

A prior study implicated the JH receptor Gce as the major receptor responsible for mating-induced infection susceptibility[9]. We sought to confirm this finding with an independent RNAi approach. Specifically, we expressed a *UAS*-controlled RNA hairpin construct targeting *gce* transcripts (*UAS-gce-RNAi*) using a knock-in driver line in which GAL4 is expressed from the endogenous *gce* locus without disrupting the native gene (*gce-T2A-GAL4*)[53], thus activating RNAi against *gce* in all cells in which *gce* is endogenously expressed. RT-qPCR analysis of adult females confirmed that this manipulation significantly reduced *gce* mRNA levels while expression of the paralogous JH receptor *Met* was unaffected (Fig. S2A).

We used this approach to ubiquitously knock down *gce* and monitored survival following *P. rettgeri* infection. We found that globally silencing *gce* fully eliminated mating-induced infection sensitivity. Mated control females, heterozygous for either the *GAL4* driver or the *UAS*-hairpin alone, succumbed to *P. rettgeri* at significantly higher rates than unmated females of the corresponding genotypes (Fig. 4A). In contrast, mated *gce* knockdown females survived infection comparably to their unmated siblings and were significantly more resistant than mated control flies (Fig. 4A). Thus, our data validate previous findings that Gce is required for the mating-induced increase in infection mortality[9].

We next asked whether Gce acts in a tissue-specific manner to reduce immune performance. The fat body regulates both immunity and reproduction in female flies[54,55], and JH signaling in the fat body promotes oogenesis[38]. We therefore hypothesized that mating-induced reduction of immune defenses might depend on Gce in the fat body. To test this, we used the *Lpp-GAL4* driver[56] to knock down *gce* expression specifically in the fat body (Fig. S2B) and recorded mortality after *P. rettgeri* infection. Consistent with our hypothesis, we found that fat-body-specific *gce* knockdown fully blocked mating-induced infection sensitivity (Fig. 4B). While mating significantly increased susceptibility to infection in driver-only control females, mated females with *gce* expression knocked down in the fat body exhibited minimal infection-induced mortality. In fact, mated *Lpp>gce-RNAi* knockdown females were moderately but significantly more resistant to *P. rettgeri* infection than unmated females of either genotype (Fig. 4B).

Knocking down *gce* in the adult fat body does not inhibit post-mating infection sensitivity

Having shown that mating activates JH signaling (Fig. 2), and that mating-induced infection sensitivity requires Gce in fat body cells (Fig. 4B), the simplest hypothesis would be that JH acts autonomously on the adult fat body through its receptor Gce to directly inhibit host immune defense. We reasoned that if this were true, then we could fully eliminate post-mating infection susceptibility by knocking down *gce* in the fat body of adult females after development is complete but prior to mating. To test this, we used the temperature-sensitive GAL80^{TS} repressor to inhibit fat-body-specific *gce* RNAi during larval and pupal development (see Materials & Methods). Then, two days after adult eclosion, we shifted virgin females to the permissive temperature to activate *gce*

knockdown in the fat body. Five days after RNAi induction, females were allowed to mate, and 24 hours later, they were infected with *P. rettgeri* (Fig. 5A row "B"). We confirmed *gce* knockdown with RT-qPCR on abdominal carcasses dissected from virgin females five days post-RNAi-induction, verifying significantly reduced *gce* expression at the exact timepoint at which females were mated (Fig. S3D). Thus, *gce* expression and function should be preserved throughout development in these experiments, but *gce* function in the fat body should be inhibited prior to and during mating and subsequent infection. Surprisingly, we found that *gce* knockdown solely in the adult fat body did not eliminate mating-induced susceptibility to infection. Knockdown and control females were both significantly more likely to die from infection when mated (Fig. 5B). Moreover, we found that adult-specific knockdown in mated females led to moderately increased mortality compared to mated driver-only controls (Fig. 5B). This result does not support the simplest model of mating-induced JH acting directly on the adult fat body through Gce, as knocking down *gce* expression only in the adult fat body does not rescue post-mating immune performance. Oppositely, *gce* function in the adult fat body seems to slightly promote infection resistance.

Next, we investigated a requirement for Gce in the fat tissue of newly-emerged adults to suppress immune defenses. JH titers spike dramatically within hours of eclosion and then gradually decline over the first three days of adulthood[57,58]. This time window coincides with final maturation of the adult fat body[59–61]. We hypothesized that Gce might play a role in fat cells shortly after eclosion, potentially transducing signals from the JH peak during this period that could ultimately enable mating to reduce infection resistance. We reasoned that this post-eclosion signaling may not have been perturbed in our

previous experiment (Fig. 5B) because *gce* knockdown was induced two days after female emergence, therefore after this spike in hormone levels has occurred.

This hypothesis predicts that knocking down *gce* in fat cells prior to eclosion and throughout early adulthood would block effects initiated by the JH peak at eclosion. If the post-eclosion JH peak were required for mating-induced infection sensitivity, then this manipulation would be sufficient to increase infection survival similarly to whole-life RNAi (Fig. 4B). To test this, we activated *gce* RNAi in the fat body beginning midway through pupal development (~P8-P10 stages), such that virgin females should eclose with *gce* already knocked down in adipocytes. We again isolated virgin females, maintained them at the RNAi-active temperature for five days, then allowed them to mate and infected them with *P. rettgeri* (Fig. 5A row "C"). This mid-pupal knockdown was not sufficient to block mating-induced infection sensitivity. Mated females with fat-body-specific *gce* knockdown were moderately less susceptible to infection than mated control females, but were still significantly more likely to die than their unmated siblings or unmated controls (Fig. 5C). Thus, we do not find evidence that the spike in JH signaling at eclosion is solely responsible for post-mating immune suppression.

Mating-induced infection sensitivity is potentiated by Gce in the pupal fat body

Our results thus far had shown that knocking down *gce* in the fat body throughout the larval, pupal, and adult stages fully blocks mating-induced infection sensitivity (Fig. 4B, Fig. 5A top row). Published work[9] found that tissue-ubiquitous *gce* knockdown from the white prepupal stage (WPP) through adulthood also prevented mating from reducing infection resistance (Fig. 5A second row). Publicly available RNA-seq data from the modENCODE database[62,63] indicate that *gce* is expressed in *D. melanogaster* fat body

tissue throughout metamorphosis and adulthood, with low but detectable transcript levels in adipocytes of wandering L3 larvae, white prepupae, mid-stage (P8) pupae, and in the carcasses (enriched for fat tissue) of 1-day-, 4-day-, and 20-day-old adult flies (Fig. S3A). We confirmed these expression patterns by crossing the *gce-T2A-GAL4* line to *UAS-RFP* and *UAS-GFP* fluorescent reporters, thus providing a visual readout of endogenous *gce* expression. We observed widespread reporter signal in fat bodies of both WPP females (Fig. S3B, B') and young adult females (Fig. S3C, C'), indicating that *gce* is expressed in the fat bodies of both pupal and adult flies. This led us to consider the possibility that Gce might function in adipocytes during metamorphosis to facilitate mating-induced infection sensitivity in adults.

Since *gce* knockdown spanning the entire pupal phase blocked mating-induced infection sensitivity (Fig. 4)[9] but knockdown initiated at the mid-pupal stage or later did not (Fig. 5B, 5C), we inferred that Gce might function in adipocytes at earlier pupal stages or throughout metamorphosis to suppress immune defenses in mated adult females. To test this, we induced fat-body-specific knockdown from the WPP stage until adult eclosion, then shifted virgin females back to 18ºC to inactivate the RNAi and allow *gce* expression to recover prior to mating and infection (Fig. 5A row "D"). We confirmed that *gce* expression in adult fat bodies was restored to control levels after releasing the knockdown in the adult (Fig. S3E). Because pathogen proliferation and consequent effects on the host may occur more slowly at lower temperatures, in this experiment we monitored survival for ten days post-infection. In contrast to the preceding experiments, we found that knocking down *gce* in the fat body solely during the pupal stages substantially mitigated mating-induced infection sensitivity. Mated females that had sustained *gce*

RNAi in the fat body during pupal stages survived *P. rettgeri* infection comparably to unmated control females and were significantly more resistant to infection than mated controls (Fig. 5D). Notably, mated knockdown females still exhibited slightly higher mortality than their unmated siblings, although the magnitude of increased death was minimal compared to that observed with driver-only control females (Fig. 5D). Thus, reducing *gce* expression in fat body cells solely during the pupal life stage can largely eliminate mating-induced sensitivity to infection, while loss of *gce* solely in the adult fat body does not enhance survival of pathogen challenge.

Mating-induced infection sensitivity is mitigated by *gce* knockdown in multiple adult tissues

In mated females JH promotes egg production[18,39,43,64], and mating does not increase infection susceptibility of *D. melanogaster* mutants that arrest oogenesis at any stage preceding vitellogenesis[4,5,8,11]. JH stimulates vitellogenin production by the fat body[36–39], and *gce* is expressed in the follicle cells of vitellogenic (stage 8-9) egg chambers[53]. Since knocking down *gce* in the adult fat body alone was not sufficient to increase survival (Fig. 5B), these observations led us to ask whether mating-induced infection sensitivity might depend on Gce function in the ovarian follicle cells, either exclusively or in combination with Gce function in the adult fat body. To address this question, we induced *gce* RNAi using the *tj-GAL4* driver, which is active in follicle cells, the adult fat body, and the brain (Fig. S4)[65,66]. We used *tj-GAL4* in conjunction with *GAL80^{TS}* to activate RNAi in fully developed adults prior to mating and *P. rettgeri* challenge (Fig. 6A).

We found that adult-specific *gce* knockdown in the follicle cells, fat body, and brain strongly increased the ability of mated females to withstand *P. rettgeri* infection. Mated

tj^{TS}>*gce-RNAi* females were significantly more resistant to infection than mated *tj-GAL4*^{TS}/+ control females and survived comparably to unmated *tj-GAL4*^{TS}/+ controls (Fig. 6B). Notably, however, *gce* knockdown in the *tj-GAL4*-targeted tissues did not completely alleviate mating-induced infection sensitivity: mated RNAi females still succumbed to infection at moderately but significantly higher rates than unmated RNAi females (Fig. 6B).

Because adult-specific *gce* knockdown in the ovary, fat body, and brain did not completely eliminate mating-induced infection susceptibility, we hypothesized that Gce function in additional tissues or cell types of adult females might contribute to reduction of immune defenses. To test this, we knocked down *gce* in all adult tissues prior to mating and infection using both the *gce-T2A-GAL4* driver to activate RNAi in the endogenous *gce* expression pattern and the strong, ubiquitous *tubulin-GAL4* driver. Both drivers were deployed in combination with GAL80^{TS} to induce *gce* RNAi in virgin females for five days after adult eclosion, before mating and infection (Fig. 6A). RT-qPCR analysis confirmed that *gce* expression levels were similar, though slightly reduced, between two-day-old *tub*^{TS}/+ control and *tub*^{TS}>*gce-RNAi* knockdown females held at 18ºC, indicating that RNAi was not active during development, and that *gce* expression was strongly diminished in the knockdown genotype compared to control females after five days of RNAi activation at 29ºC (Fig. S3F).

Unlike adult-specific RNAi localized only to the fat body only (Fig. 5B) or to the fat body, ovary, and brain in combination (Fig. 6B), tissue-ubiquitous, adult-specific *gce* knockdown with either driver fully blocked mating-induced infection sensitivity. Mated females with adult-specific *gce* RNAi induced by *gce-T2A-GAL4* or *tub-GAL4* survived

infection with *P. rettgeri* equivalently to their unmated siblings, in contrast to the strong mating-induced infection susceptibility observed with *gce-T2A-GAL4^{TS}/+* and *tub-GAL4^{TS}/+* control females (Fig. 6C, D). Furthermore, we found that adult-specific knockdown with the *gce-T2A-GAL4* driver enhanced resistance to infection irrespective of mating status, with both unmated and mated RNAi females surviving more than even unmated control females (Fig. 6C).

DISCUSSION

Based on our collective findings, we propose a model wherein JH and the JH receptor Gce suppress immune defenses by regulating both developmental processes during metamorphosis and dynamic post-mating responses in adult females (Fig. 7). Our data suggest that Gce first acts in pupal fat cells during metamorphic development, with the consequence that developing adult females become sensitized to future immune-suppressive effects of mating. In the adult stage, mating stimulates a rapid peak in circulating JH levels that subsides within hours but stabilizes at levels that remain consistently elevated for days. We propose that the steady presence of JH in the hemolymph continuously suppresses immunity via the action of Gce in the fat body and other tissues including the ovarian follicle cells.

In adult *D. melanogaster*, systemic bacterial infections induce massive transcriptional upregulation of genes encoding antimicrobial peptides (AMPs) in the fat body[67–69] and JH has been shown to attenuate this induction[9,29]. Additionally, JH promotes expression of yolk protein genes in the fat body[36–39] and prior work has suggested yolk production contributes to post-mating immune suppression[8], potentially by diverting cellular resources from the immune response. From these observations, the

simplest hypothesis would have been that mating-induced JH/Gce signaling would reduce immune performance entirely by autonomously suppressing AMP expression and/or promoting expression of resource-consuming molecules like vitellogenins in the adult fat body. However, our evidence does not support this simple model. Instead, our findings suggest that JH-induced infection sensitivity is initially potentiated during metamorphosis and subsequently requires mating-induced signaling in the adult. Our data are consistent with a model wherein mating activates a complex, JH-dependent signaling network in the adult, resulting in tissue autonomous and non-autonomous suppression of immune function of the fat body, at least partially regulated through Gce action in the follicle cells and possibly other tissues (Fig 7). Alternatively, Gce might primarily act non-autonomously in the follicle cells to affect fat body immune function, and the differences in magnitude of phenotype suppression we observed between ubiquitous- and *tj-GAL4*-induced *gce* RNAi could be due to differences in driver strength. The full post-mating response could also involve additional tissues that we did not resolve in the present study, such as the ovarian muscle sheath, in which JH signaling was recently shown to promote oocyte development and ovulation[38], or other somatic cells with major immune functions, such as the hemocytes or oenocytes. Additionally, Gce in the central nervous system (which could have been disrupted by RNAi driven by *tj-GAL4* in our study) might affect neuroendocrine functions that systemically control metabolism or oogenesis, thus indirectly constraining immunity. Future determination of the transcriptional targets of Gce across distinct cell types and life stages will reveal key molecular functions that underlie the complex effects of JH signaling on immune function and infection resistance.

Our findings reveal a previously unrecognized contribution of JH developmental functions to mediating the antagonistic relationship between reproduction and immunity. This effect might be partially attributable to functional interactions with the steroid hormone 20-hydroxyecdysone (20E). In larvae, interactions between JH and 20E have been shown to control key aspects of fat body development. At the onset of pupation, a subset of larval adipocytes undergoes apoptosis and the larval fat body fragments, processes known to be regulated by the balance of JH and 20E[43,70–72]. During metamorphosis, the adult fat body forms from an independent, mesoderm-derived cellular lineage[60,61]. While 20E has been implicated in adult fat body formation[61], a role for JH has not been described. Based on our findings, Gce might act in the fragmenting larval fat tissue, adult fat body precursor cells, or potentially both of these adipocyte populations, shaping how the adult fat body will respond to future stimuli like mating-induced endocrine activity and pathogenic infection. Notably, JH III titers are reported low-to-undetectable during these pupal stages[57,58], so Gce function in these cell populations may be responsive to ligands like JHB3 or methyl farnesoate[73]. Alternatively, Gce might control fat body metamorphosis via ligand-independent interactions with known binding partners like 14-3-3 proteins or the nuclear receptor Ftz-F1[74,75], both of which have been implicated as immune regulators[76,77]. Importantly, while our findings suggest an important function for Gce in pupal adipocytes, this does not rule out the possibility that JH/Gce might also regulate the metamorphic or early adult development of other organs – for example promoting ovarian maturation[39,78,79] – in ways that potentiate subsequent post-mating immune suppression in adult females.

At the end of the larval growth period, a drop in JH titers and corresponding peak in 20E titers initiates metamorphic cellular programs[80]. This includes the pronounced, 20E-dependent transcriptional upregulation of innate immune genes at pupariation, which has been proposed to guard the animal against microbes released from the gut as larval tissues undergo histolysis[81–85]. Recent work has shown that this activation of immune pathways in early pupae is necessary for age-dependent upregulation of antimicrobial peptides[85] and resistance to viral infection[86] in adults. These findings are similar to our observations that Gce function in pupal adipocytes suppresses adult antibacterial defenses. This developmental immune induction may occur through upstream activation of the NF-κB pathways that control humoral immunity[85,86], or through direct regulation of AMP-encoding genes by hormone-regulated transcription factors[81]. Gce could potentially influence both of these mechanisms via functional interactions with the 20E network. While the mechanisms by which immune gene induction during pupariation shapes adult immune traits remain unknown, our work suggests Gce might contribute to the regulatory mechanisms that control this pupal-specific immune activity with consequences for later infection responses.

Prior work has shown that a single mating is sufficient to induce lasting immune suppression[5,7], and our results in the present study indicate that a single mating also induces JH signaling activity sustained over several days. This underscores the importance of JH as a key endocrinological driver of major, lasting shifts in female physiological states induced by mating, which include impaired immune defenses. Interestingly, the persistent JH signaling we observed occurs despite relatively low levels of JH III following an initial post-mating peak in hormone titers. The initial JH transduction

may induce positive feedback mechanisms that increase sensitivity to subsequently limited ligand levels. These mechanisms could include increasing *gce/Met* expression levels, or the expression of co-regulators that stabilize or enhance JH receptor potency. This increased sensitivity would be consistent with our finding that a continual source of JH appears to be necessary for sustained immune suppression, while a single pulse of JH signal activation is not sufficient to increase infection sensitivity. These observations do not support a mechanism wherein mating-induced JH signaling contributes to long-lasting immune suppression by causing permanent, irreversible changes to organ states, such as structural or functional tissue remodeling. Rather, our findings are more consistent with the possibility that sustained JH signaling drives biological responses, such as mechanisms proposed above, that actively and continuously reduce immune defenses.

JH is a deeply conserved insect hormone that has long been recognized to pleiotropically regulate many aspects of insect biology. Notably, the effect of JH on immunity appears to vary among insect species. As we observe in *D. melanogaster*, JH has been shown to be immunosuppressive in *Tribolium castaneum*[21], *Tenebrio molitor*[25], *Spodoptera exigua*[22,87], and *Hetaerina americana*[23]. In contrast, JH appears to promote expression of immune related genes in the fat body of *Bombyx mori* larvae[24]. In the mosquito *Aedes aegypti*, studies have indicated that JH may either promote[27] or suppress[26] antibacterial humoral immunity, while activating antiviral[88] and cellular immune defenses[27]. Thus, while the vital developmental and gonadotropic functions of JH are conserved across taxa, the impact of JH on immunity may be more plastic and, potentially, dependent on specific life history strategies. One intriguing possibility is that

the differing effects of JH on immunity in these organisms could be partly attributable to differences in JH signaling dynamics that sustain their varied modes of development and reproduction.

Our study implicates JH as a key factor that shapes the physiological balance among immunity, reproduction, and development. Determining exactly how development of the adult fat body is shaped by JH/Gce during metamorphosis – and how that potentiates subsequent adult sensitivity to post-mating JH signaling and infection – is a critical next mechanistic question. Similarly, the precise role of JH/Gce in establishing homeostatic immunological and reproductive balance across adult tissues remains to be defined. Addressing these questions will advance our understanding of the ways hormones pleiotropically govern immune system performance and host-microbe interactions within the context of overall animal physiology.

MATERIALS & METHODS

D. melanogaster stocks and husbandry

The following fly stocks were used in this study: Canton-S (Bloomington *Drosophila* Stock Center stock 64349), *y*w*;;8xJHRE-eGFP* and *y*w*;;Mut8xJHRE-eGFP* [51], *w*,gce-T2A-GAL4* (BDSC 76347)[53], *w*;;Lpp-GAL4* [56], *w*;tubP-GAL80^{TS};Lpp-GAL4* [89], *w*;tubP-GAL80^{TS};tubP-GAL4* (BDSC 86328), *w*,gce-T2A-GAL4;tubP-GAL80^{TS}*, *y*w*;tj-GAL4,tubP-GAL80^{TS}* [90], *y^{1}v^{1};attP40* (BDSC 36304), *y^{1}v^{1};UAS-gce-RNAi^{HMJ23341}* (BDSC 61852), *w*;UAS-GFP.nls*, *w^{1118};UAS-RFP.W* (BDSC 30556).

Flies were cultured on a diet of the following composition (weight-per-volume or volume-per-volume): 6% cornmeal, 6% yeast, 4% sucrose, 0.7% agar, 0.265% methylparaben, 0.05% phosphoric acid, and 0.5% propionic acid. Flies were housed in groups of 10-20

animals per vial and maintained on a 12H:12H light:dark cycle. Experiments were conducted at 25ºC, except for temperature-controlled RNAi experiments described below.

Information on fly stocks and transgenes, and modENCODE gene expression data were obtained from FlyBase (release FB2025_02)[91].

Mating procedures

For experiments testing the effects of mating, females were collected within 6 hours of eclosion under light CO_2 anesthesia and isolated in food vials in groups of 10-20 individuals per vial. One subset of collected females was maintained as virgins while another subset was allowed to mate according to the procedure detailed below. Thus, for each genotype in an experimental replicate, mated and unmated females were siblings reared under the same conditions.

Females of all genotypes used in the study were mated with Canton-S males aged 5-7 days post-eclosion. For each vial of females to be mated in an experiment, a group of 10-15 Canton-S males was isolated ~24 hours in advance to allow full recovery from CO_2 anesthesia prior to mating. On the day of the experiment, males were transferred into vials containing unmated females. All females were observed to copulate within 30 min of introducing males.

Data presented in Figs. 1A, 1B, Fig. 2, and Fig. S1 were collected from females analyzed at specific times post-mating. For these experiments, females and males were initially housed together and allowed to mate for 30 min. The females were then separated under light CO_2 anesthesia and placed in vials for the prescribed length of time prior to data collection. To control for any effects of this brief CO_2 exposure, unmated females were anesthetized for a similar amount of time. For all other experiments, females were

co-housed with males for 24 hours prior to administering infections (see details below), at which point males were discarded. Infected females were housed in food vials without males for subsequent survival analyses.

JH III exposure

Unmated female flies were treated with JH III using filter paper saturated with a volatilized hormone solution. Semicircular discs of Grade 1 Whatman filter paper (2.5 cm diameter; Sigma 1001-150) were placed in standard *Drosophila* food vials that had been left uncapped in a fume hood for ~1-3 hours to allow evaporation of excess moisture. JH III (Sigma J2000) was reconstituted in methanol to a 5 µg/µL stock solution, then diluted in acetone to the indicated concentrations. Control solution was prepared by mixing an equivalent volume of methanol in acetone. All solutions were prepared in silanized glass vials (Thermo Scientific C4000-S2W) to prevent JH III adsorption[92]. To initiate exposure, 10µL of JH III or control solution was pipetted directly onto the filter paper immediately before transferring flies to exposure vials. Females were flipped into new exposure vials with freshly prepared JH III solution every 24 hours.

Liquid chromatography-tandem mass spectrometry quantification of JH III titers

JH III levels were quantified according to published protocols[20,93] with modifications.

Juvenile hormone extraction

For JH extraction, 50 flies per sample were homogenized in 400 µL of ice-cold methanol containing 10 ppm deuterated JH III (JH III-D3) as an internal standard. To this, 100 µL of 2% sodium chloride solution was added, followed by 300 µL of hexane. The samples were vortexed for 1 minute and then centrifuged at 845 x g for 5 min at 4ºC. After centrifugation, ~300 µL of the top hexane layer was transferred to a silanized glass vial.

Hexane extraction was repeated twice, and all fractions were pooled in a single vial. These samples were dried and stored at -80ºC until LC-MS/MS based quantitation.

Sample Preparation for LC-MS/MS

Dried samples were reconstituted in 500 µL 100% methanol, vortexed for 10 sec, and stored overnight at -20ºC. Samples were sonicated for 10 min, vortexed (1800 rpm, 15 min, room temperature), and transferred to 1.5 mL microcentrifuge tubes. The original vial was rinsed with an additional 200 µL 100% methanol, and the rinse was combined with the extract (total volume ~700 µL). Samples were centrifuged at 16,000 x g for 15 min at 4ºC. Approximately 675 µL of supernatant was transferred to clean tubes and evaporated in a speed vacuum concentrator. The resulting brown, gel-like pellets were stored at -20ºC until MS analysis. Prior to analysis, samples were reconstituted in 100 µL of 100% methanol (without formic acid to avoid diol formation), vortexed (1800 rpm, 15 min, room temperature), and centrifuged at 16,000 x g for 15 min at 4ºC. A 40 µL aliquot was transferred to autosampler vials maintained at 4ºC.

Liquid Chromatography

LC-MS/MS analysis was conducted at the Proteomics and Metabolomics Facility of the Cornell Institute of Biotechnology (RRID:SCR_021743). Chromatographic separation was performed using an ExionLC™ system (SCIEX) equipped with a Luna C18(2) column (100 mm × 2.0 mm i.d., 3 µm; Phenomenex). The column temperature was maintained at 30°C, and the flow rate was set at 300 µL/min. The mobile phases consisted of (A) 0.1% formic acid and (B) 100% acetonitrile. A gradient elution program was applied over 15 min. The injection volume was 10 µL for standards and 10-40 µL for samples, using a 50 µL loop volume.

Mass Spectrometry

Mass spectrometric analyses were performed using a SCIEX X500B quadrupole time-of-flight (QTOF) mass spectrometer operated in positive electrospray ionisation (ESI) mode.

Instrument calibration was conducted using a positive calibrant solution with the CDS system. Ion source parameters were as follows: ion spray voltage, 5.5 kV; ion source gas 1 and 2, 20 psi; curtain gas, 20 (arbitrary units); collision gas (CAD), 7 (arbitrary units); source temperature, 125°C; declustering potential (DP), 50 V; accumulation time, 0.15 s. Guided MRM high-resolution (MRM-HR) acquisition was performed by injecting 1 mg/mL individual analyte infusions (9 µL/min) diluted 20-fold with a 200 µL/min flow rate. Data acquisition consisted of a full MS scan (m/z 50–500, profile mode), followed by MRM-HR scans (three transitions per analyte) over a 15 min run time.

Data Analysis

Data acquisition and processing were performed using SCIEX OS software (version 1.7) for compound identification and quantitation. To statistically compare JH III measurements, we first assessed data normality with Shapiro-Wilk test and homogeneity of variance with Levene's test. JH III data from both experiments in the study (Fig. 2A, Fig. 3B) did not meet parametric test assumptions so were analyzed by Kruskal-Wallis test. Analysis of the data presented in Fig. 2A indicated a significant effect of time post-mating (Kruskal-Wallis $p<0.05$) so post-hoc pairwise comparisons were conducted using Dunn's test.

Development- and time-restricted *gce* RNAi

The *GAL4-UAS* system was used to reduce *gce* expression in specific tissues and cell types, or at particular developmental stages, via RNAi. Female flies carrying a transgene comprising *UAS* sites upstream of RNA hairpin sequence targeting *gce* mRNA ("*UAS-gce-RNAi*") were crossed with male flies carrying the indicated *GAL4* driver transgene to produce F1 progeny heterozygous for both genetic elements. In these progeny, GAL4 activates expression of the *UAS-gce-RNAi* construct, leading to RNAi-mediated reduction of endogenous *gce* transcript levels. To obtain genetically-matched control flies carrying the *GAL4* transgene with no *UAS* construct, we crossed *GAL4* lines to the "*attP40*" background stock in which the *UAS-gce-RNAi* line was generated. As additional controls for the experiments described in Fig. 4A, we crossed the *UAS-gce-RNAi* line with w^{1118} flies to produce females heterozygous for the *UAS* construct but lacking a driver transgene.

For the experiments illustrated in Figs. 5 and 6, we controlled the timing and duration of *gce* knockdown using GAL80^{TS} [94]. Flies carrying the ubiquitously expressed *tubP-GAL80^{TS}* transgene and the indicated GAL4 driver were crossed with *UAS-gce-RNAi* flies. Progeny of these crosses were reared at 18ºC, the permissive temperature at which GAL80^{TS} inhibits GAL4 activity and consequent *UAS* RNAi transgene expression. At the indicated developmental stages (white prepupae, mid-pupal stage, 2 day old adult virgins), flies were shifted to the restrictive temperature of 29ºC to inactivate GAL80^{TS} and de-repress GAL4-mediated induction of *UAS-gce-RNAi*. Driver-only controls were again generated by crossing flies carrying the *GAL4* and *tubP-GAL80^{TS}* transgenes to the genetically matched *attP40* background stock. These control flies were subjected to temperature shifts in parallel to the experimental knockdown flies.

Systemic infections and survival analysis

Flies were systemically infected with *Providencia rettgeri* strain Dmel [48] according to previously described protocols [95]. Bacterial cultures were grown in Luria-Bertani (LB) broth (BD Biosciences 24460) at 37ºC with shaking. Overnight cultures were pelleted by centrifugation at 10509 x g for 3 min, resuspended in sterile phosphate-buffered saline (PBS; Sigma P4417), and standardized to optical density OD_{600}=1. To administer infections, flies were briefly anesthetized on CO_2 platforms. A 0.15mm minutien pin (Fine Science Tools 26002-10) was dipped in the bacterial inoculum and flies were pricked in the sternopleural region of the thorax. To quantify bacterial doses administered with each infection, 4-8 flies were infected and immediately homogenized in 150µL PBS. Homogenate was spread on LB agar with a Whitley Automated Spiral Plater 2 (Don Whitley Scientific) and plates were incubated at 37ºC overnight. Resulting colonies were counted with a ProtoCOL3 plate counter (Microbiology International) to estimate the infectious dose introduced to each fly. Infections in this study administered ~300 colony forming units per fly.

Infected flies were housed in groups of 10-20 animals per vial and flipped to fresh food every other day. To quantify infection-induced mortality, the number of dead flies in each vial was counted daily for five days post-infection.

Infection survival data were analyzed with the “survival” package in R version 4.5.2. We used a Cox proportional hazards model to test for the effects of mating, genotype, and mating x genotype interaction, followed by Benjamini Hochberg-adjusted pairwise comparisons with the pairwise_survdiff function in the “survminer” package [96].

RT-qPCR

Whole flies or dissected abdominal carcasses/fat bodies were homogenized in 500μL Trizol reagent (Invitrogen 15596026) by bead-beating for 30 seconds with 2.3mm zirconia/silica beads (BioSpec Products 11079125z). RNA was extracted using the Zymo Research Direct-zol RNA miniprep kit (R2052) and cDNA was synthesized from 500ng RNA template with qScript cDNA SuperMix (QuantaBio 95048). qPCR was performed with PerfeCTa SYBR Green FastMix (QuantaBio 95072) on a Bio-Rad CFX Connect thermocycler. Expression levels were calculated as ΔΔCt values:

1) For each sample, Ct values of the housekeeping gene *Rpl32* were subtracted from Ct values of the gene of interest: $\Delta Ct_{GOI}=Ct_{GOI} - Ct_{Rpl32}$.

2) Experimental genotypes/treatments were normalized to control genotypes/treatments by first averaging the ΔCt values for the control group and then subtracting this average value from the ΔCt values of each individual experimental sample: $\Delta\Delta Ct_{GOI}=\Delta Ct_{experimental\_sample} - average(\Delta Ct_{control\_samples})$.

The following primers were used (all sequences 5'-3'):

Rpl32: forward CGCTTCAAGGGACAGTATCTG; reverse AAACGCGGTTCTGCATGA

eGFP: forward GAACCGCATCGAGCTGAA; reverse TGCTTGTCGGCCATGATATAG

gce: forward AGCTGCGTATCCTGGACACT; reverse TCGAGAGCTGAAACATCTCCAT

Met: forward GCCTCAAGGGAACGGGTATG; reverse AGCAGTTGCATTAGAGTGTCC

RT-qPCR data were analyzed by unpaired two-sample t-test, with a significance threshold of $p<0.05$.

Tissue staining and imaging

Expression patterns of *gce-T2A-GAL4* and *tj-GAL4* were visualized by crossing these driver lines to flies carrying *UAS-RFP* or *UAS-GFP* reporter constructs and imaging

live fluorescent signal in female F1 cross progeny. Pupal and adult fat bodies (Fig. S3B-C', Fig. S4B, B'), adult brains (Fig. S4A, A'), and ovaries (Fig. S4C, C') were dissected in ice-cold PBS and immediately fixed for 30 min at room temperature in 4% paraformaldehyde-PBS (Electron Microscopy Sciences 157-8-100). Tissues were rinsed three times with PBS + 0.3% Triton X-100 (Sigma X100) and nuclei were stained with DAPI (1µg/mL in PBS; Invitrogen D1306) for 15 min at room temperature. Tissues were washed three times with PBS and mounted in ProLong Glass Antifade Mountant (Invitrogen P36980).

Epifluorescence images were acquired on a Leica DM5000B upright microscope with a CTR5000 controller, EL6000 light source, and DFC365 FX camera using LAS AF 2.6 software.

Acknowledgements

We thank Dr. Lacy Barton for sharing *8xJHRE-eGFP* and *Mut8xJHRE-eGFP* fly stocks. We thank Dr. Deepika Vasudevan for sharing *tj-GAL4,tubP-GAL80^{TS}* flies. Stocks obtained from the Bloomington *Drosophila* Stock Center (NIH P40OD018537) were used in this study. Content from BioRender.com was used in Figure 7.

Author contributions

S.A.K., V.G., and B.P.L. designed the project and experiments. S.A.K., V.G., and A.A.K. performed the experiments. S.A.K. analyzed the data and generated the figures. S.A.K. and B.P.L. wrote the manuscript. All authors reviewed the manuscript.

Data availability

The datasets generated during and/or analyzed during the current study are available from the corresponding author on reasonable request.

Funding

This study was supported by National Institutes of Health (NIH) grant R01 AI141385 awarded to BPL. SAK was supported by NIH grant T32 AI145821.

Competing interests

The authors declare no competing interests.

References

1. Martin, L. B., Weil, Z. M. & Nelson, R. J. Seasonal changes in vertebrate immune activity: mediation by physiological trade-offs. *Philos. Trans. R. Soc. Lond. B Biol. Sci.* **363**, 321–39 (2008).
2. Norris, K. & Evans, M. R. Ecological immunology: life history trade-offs and immune defense in birds. *Behavioral Ecology* **11**, 19–26 (2000).
3. Schwenke, R. A., Lazzaro, B. P. & Wolfner, M. F. Reproduction-Immunity Trade-Offs in Insects. *Ann. Rev. Entomol.* **61**, 239–256 (2016).
4. Short, S. M. & Lazzaro, B. P. Reproductive status alters transcriptomic response to infection in female *Drosophila melanogaster*. *G3 (Genes, Genomes, Genetics)* **3**, 827–40 (2013).
5. Short, S. M., Wolfner, M. F. & Lazzaro, B. P. Female *Drosophila melanogaster* suffer reduced defense against infection due to seminal fluid components. *J. Insect Physiol.* **58**, 1192–1201 (2012).
6. Short, S. M. & Lazzaro, B. P. Female and male genetic contributions to post-mating immune defence in female *Drosophila melanogaster*. *Proceedings of the Royal Society B: Biological Sciences* **277**, 3649–3657 (2010).
7. Gordon, K. E., Wolfner, M. F. & Lazzaro, B. P. A single mating is sufficient to induce persistent reduction of immune defense in mated female *Drosophila melanogaster*. *J. Insect Physiol.* **140**, 104414 (2022).
8. Gordon, K. E. *et al.* Trade-off between antibacterial immune defense and oogenesis progression in female *Drosophila melanogaster*. *Genetics* **231**, iyaf151 (2025).
9. Schwenke, R. A. & Lazzaro, B. P. Juvenile Hormone Suppresses Resistance to Infection in Mated Female *Drosophila melanogaster*. *Current Biology* **27**, 596–601 (2017).
10. Gupta, V., Frank, A. M., Matolka, N. & Lazzaro, B. P. Inherent constraints on a polyfunctional tissue lead to a reproduction-immunity tradeoff. *BMC Biol.* **20**, 127 (2022).
11. Fedorka, K. M., Linder, J. E., Winterhalter, W. & Promislow, D. Post-mating disparity between potential and realized immune response in *Drosophila melanogaster*. *Proc. Biol. Sci.* **274**, 1211–7 (2007).

12. Wigby, S., Domanitskaya, E. V, Choffat, Y., Kubli, E. & Chapman, T. The effect of mating on immunity can be masked by experimental piercing in female *Drosophila melanogaster*. *J. Insect Physiol.* **54**, 414–20 (2008).

13. Singh, A. *et al.* Experimental adaptation to singular pathogen challenge reduces susceptibility to novel pathogens in *Drosophila melanogaster*. *Current Research in Insect Science* **7**, 100105 (2025).

14. Shianiou, G., Teloni, S. & Apidianakis, Y. Intestinal Immune Deficiency and Juvenile Hormone Signaling Mediate a Metabolic Trade-off in Adult *Drosophila* Females. *Metabolites* **13**, 340 (2023).

15. Adhikari, K. & Lazzaro, B. P. Reciprocal costs of infection and reproduction in *Drosophila melanogaster*. *Biol. Lett.* **21**, 20240475 (2025).

16. Adhikari, K., Ali, F., Malo, M. A. & Lazzaro, B. P. Ovariole number does not predict reproductive output or trade-off with immunity in *Drosophila melanogaster*. *PLoS One* **20**, e0333046 (2025).

17. Roy, S., Saha, T. T., Zou, Z. & Raikhel, A. S. Regulatory Pathways Controlling Female Insect Reproduction. *Annu. Rev. Entomol.* **63**, 489–511 (2018).

18. Reiff, T. *et al.* Endocrine remodeling of the adult intestine sustains reproduction in *Drosophila*. *Elife* **4**, e06930 (2015).

19. Moshitzky, P. *et al.* Sex-peptide activates juvenile hormone biosynthesis in the *Drosophila melanogaster* corpus allatum. *Arch. Insect Biochem. Physiol.* **32**, 363–74 (1996).

20. Sugime, Y. *et al.* Upregulation of Juvenile Hormone Titers in Female *Drosophila melanogaster* Through Mating Experiences and Host Food Occupied by Eggs and Larvae. *Zoolog. Sci.* **34**, 52–57 (2017).

21. Hepat, R. & Kim, Y. JH modulates a cellular immunity of *Tribolium castaneum* in a Met-independent manner. *J. Insect Physiol.* **63**, 40–7 (2014).

22. Kim, Y., Jung, S. & Madanagopal, N. Antagonistic effect of juvenile hormone on hemocyte-spreading behavior of *Spodoptera exigu*a in response to an insect cytokine and its putative membrane action. *J. Insect Physiol.* **54**, 909–15 (2008).

23. González-Tokman, D. M., Munguía-Steyer, R., González-Santoyo, I., Baena-Díaz, F. S. & Córdoba-Aguilar, A. Support for the immunocompetence handicap hypothesis in the wild: hormonal manipulation decreases survival in sick damselflies. *Evolution (N. Y).* **66**, 3294–301 (2012).

24. Tian, L. *et al.* Genome-wide regulation of innate immunity by juvenile hormone and 20-hydroxyecdysone in the *Bombyx* fat body. *BMC Genomics* **11**, 549 (2010).

25. Rolff, J. & Siva-Jothy, M. T. Copulation corrupts immunity: a mechanism for a cost of mating in insects. *Proc. Natl. Acad. Sci. U. S. A.* **99**, 9916–8 (2002).

26. Chang, M.-M. *et al.* Regulation of antimicrobial peptides by juvenile hormone and its receptor, Methoprene-tolerant, in the mosquito *Aedes aegypti*. *Insect Biochem. Mol. Biol.* **128**, 103509 (2021).

27. Kim, I. H. *et al.* A mosquito juvenile hormone binding protein (mJHBP) regulates the activation of innate immune defenses and hemocyte development. *PLoS Pathog.* **16**, e1008288 (2020).

28. Kwon, S. & Kim, Y. Immunosuppressive action of pyriproxyfen, a juvenile hormone analog, enhances pathogenicity of *Bacillus thuringiensis* subsp. *kurstaki* against diamondback moth, *Plutella xylostella* (Lepidoptera: Yponomeutidae). *Biological Control* **42**, 72–76 (2007).

29. Flatt, T. *et al.* Hormonal regulation of the humoral innate immune response in *Drosophila melanogaster*. *Journal of Experimental Biology* **211**, 2712–2724 (2008).

30. Riddiford, L. M. Rhodnius, Golden Oil, and Met: A History of Juvenile Hormone Research. *Front. Cell Dev. Biol.* **8**, 679 (2020).

31. Flatt, T., Tu, M. P. & Tatar, M. Hormonal pleiotropy and the juvenile hormone regulation of *Drosophila* development and life history. *BioEssays* **27**, 999–1010 (2005).

32. Shalem, Y., Goldberg, T. S. & Bloch, G. Juvenile hormone signaling and social complexity in the Hymenoptera. *Curr. Opin. Insect Sci.* **72**, 101433 (2025).

33. Krishnan, N. Endocrine Control of Lipid Metabolism. *Adv. Exp. Med. Biol.* **1494**, 201–216 (2026).

34. Jindra, M., Palli, S. R. & Riddiford, L. M. The juvenile hormone signaling pathway in insect development. *Annu. Rev. Entomol.* **58**, 181–204 (2013).

35. Santos, C. G., Humann, F. C. & Hartfelder, K. Juvenile hormone signaling in insect oogenesis. *Curr. Opin. Insect Sci.* **31**, 43–48 (2019).

36. Jowett, T. & Postlethwait, J. H. The regulation of yolk polypeptide synthesis in *Drosophila* ovaries and fat body by 20-hydroxyecdysone and a juvenile hormone analog. *Dev. Biol.* **80**, 225–234 (1980).

37. Bownes, M. & Blair, M. The Effects of a Sugar Diet and Hormones on the Expression of the *Drosophila* Yolk-Protein Genes. *J. Insect Physiol.* **32**, 493-501 (1986).

38. Luo, W. *et al.* Juvenile hormone signaling promotes ovulation and maintains egg shape by inducing expression of extracellular matrix genes. *Proc. Natl. Acad. Sci. U. S. A.* **118**, e2104461118 (2021).

39. Yamamoto, R., Bai, H., Dolezal, A. G., Amdam, G. & Tatar, M. Juvenile hormone regulation of *Drosophila* aging. *BMC Biol.* **11**, 85 (2013).

40. Hiruma, K. & Kaneko, Y. Hormonal regulation of insect metamorphosis with special reference to juvenile hormone biosynthesis. *Curr. Top. Dev. Biol.* **103**, 73–100 (2013).

41. Jindra, M., Tumova, S., Bittova, L., Tuma, R. & Sedlak, D. Agonist-dependent action of the juvenile hormone receptor. *Curr. Opin. Insect Sci.* **65**, 101234 (2024).

42. Jindra, M., Tumova, S., Milacek, M. & Bittova, L. Chapter Two - A decade with the juvenile hormone receptor. in *Advances in Insect Physiology* (ed. Adams, M. E.) vol. 60 37–85 (Academic Press, 2021).

43. Abdou, M. A. *et al. Drosophila* Met and Gce are partially redundant in transducing juvenile hormone action. *Insect Biochem. Mol. Biol.* **41**, 938–45 (2011).

44. Jindra, M., Uhlirova, M., Charles, J.-P., Smykal, V. & Hill, R. J. Genetic Evidence for Function of the bHLH-PAS Protein Gce/Met As a Juvenile Hormone Receptor. *PLoS Genet.* **11**, e1005394 (2015).

45. Baumann, A., Fujiwara, Y. & Wilson, T. G. Evolutionary divergence of the paralogs Methoprene tolerant (Met) and germ cell expressed (gce) within the genus *Drosophila*. *J. Insect Physiol.* **56**, 1445–55 (2010).

46. Wilson, T. G. & Fabian, J. A *Drosophila melanogaster* mutant resistant to a chemical analog of juvenile hormone. *Dev. Biol.* **118**, 190–201 (1986).

47. Jindra, M. & Bittova, L. The juvenile hormone receptor as a target of juvenoid 'insect growth regulators'. *Arch. Insect Biochem. Physiol.* **103**, e21615 (2020).

48. Juneja, P. & Lazzaro, B. P. *Providencia sneebia sp. nov.* and *Providencia burhodogranariea sp. nov.*, isolated from wild *Drosophila melanogaster*. *Int. J. Syst. Evol. Microbiol.* **59**, 1108–1111 (2009).

49. Minakuchi, C., Namiki, T. & Shinoda, T. Krüppel homolog 1, an early juvenile hormone-response gene downstream of Methoprene-tolerant, mediates its anti-metamorphic action in the red flour beetle *Tribolium castaneum*. *Dev. Biol.* **325**, 341–50 (2009).

50. Dubrovsky, E. B., Dubrovskaya, V. A. & Berger, E. M. Juvenile hormone signaling during oogenesis in *Drosophila melanogaster*. *Insect Biochem. Mol. Biol.* **32**, 1555–65 (2002).

51. Barton, L. J. *et al.* Juvenile hormones direct primordial germ cell migration to the embryonic gonad. *Current Biology* **34**, 505-518.e6 (2024).

52. Kurogi, Y. *et al.* The seminal vesicle is a juvenile hormone-responsive tissue in adult male *Drosophila melanogaster*. *Open Biol.* **14**, 240315 (2024).

53. Baumann, A. A. *et al.* Genetic tools to study juvenile hormone action in *Drosophila*. *Sci. Rep.* **7**, 2132 (2017).

54. Arrese, E. L. & Soulages, J. L. Insect fat body: Energy, metabolism, and regulation. *Annu. Rev. Entomol.* **55**, 207–225 (2010).

55. Li, S., Yu, X. & Feng, Q. Fat Body Biology in the Last Decade. *Annu. Rev. Entomol.* **64**, 315–333 (2019).

56. Brankatschk, M. & Eaton, S. Lipoprotein particles cross the blood-brain barrier in *Drosophila*. *J. Neurosci.* **30**, 10441–10447 (2010).

57. Bownes, M. & Rembold, H. The titre of juvenile hormone during the pupal and adult stages of the life cycle of *Drosophila melanogaster*. *Eur. J. Biochem.* **164**, 709–12 (1987).

58. Zhang, S. X., Glantz, E. H., Miner, L. E., Rogulja, D. & Crickmore, M. A. Hormonal control of motivational circuitry orchestrates the transition to sexuality in *Drosophila*. *Sci. Adv.* **7**, eabg6926 (2021).

59. Johnson, M. B. & Butterworth, F. M. Maturation and aging of adult fat body and oenocytes in *Drosophila* as revealed by light microscopic morphometry. *J. Morphol.* **184**, 51–59 (1985).

60. Lei, Y. *et al.* FGF signaling promotes spreading of fat body precursors necessary for adult adipogenesis in *Drosophila*. *PLoS Biol.* **21**, e3002050 (2023).

61. Tsuyama, T., Hayashi, Y., Komai, H., Shimono, K. & Uemura, T. Dynamic *de novo* adipose tissue development during metamorphosis in *Drosophila melanogaster*. *Development* **150**, dev200815 (2023).

62. Brown, J. B. *et al.* Diversity and dynamics of the *Drosophila* transcriptome. *Nature* **512**, 393–9 (2014).

63. modENCODE Consortium *et al.* Identification of functional elements and regulatory circuits by *Drosophila* modENCODE. *Science* **330**, 1787–97 (2010).

64. Gruntenko, N. E. *et al.* Altered juvenile hormone metabolism, reproduction and stress response in *Drosophila* adults with genetic ablation of the corpus allatum cells. *Insect Biochem. Mol. Biol.* **40**, 891–7 (2010).

65. Weaver, L. N., Ma, T. & Drummond-Barbosa, D. Analysis of Gal4 Expression Patterns in Adult *Drosophila* Females. *G3 (Genes, Genomes, Genetics)* **10**, 4147–4158 (2020).

66. Zike, A. B., Abel, M. G., Eisman, R. C. & Weaver, L. N. Adipocyte-Derived Amino Acid Storage Proteins are Required for Germline Stem Cell Maintenance in Adult *Drosophila* Females. *Dev. Biol.* **534**, 61-73 (2026).

67. Tzou, P. *et al.* Tissue-specific inducible expression of antimicrobial peptide genes in *Drosophila* surface epithelia. *Immunity* **13**, 737–748 (2000).

68. Westlake, H., Hanson, M. A. & Lemaitre, B. *The Drosophila Immunity Handbook*. Lausanne, Switzerland: EPFL Press (2025).

69. Vaibhvi, V., Künzel, S. & Roeder, T. Hemocytes and fat body cells, the only professional immune cell types in *Drosophila*, show strikingly different responses to systemic infections. *Front. Immunol.* **13**, 040510 (2022).

70. Liu, Y. *et al.* Juvenile hormone counteracts the bHLH-PAS transcription factors MET and GCE to prevent caspase-dependent programmed cell death in *Drosophila*. *Development* **136**, 2015–25 (2009).

71. Postlethwait, J. H. & Jones, G. J. Endocrine control of larval fat body histolysis in normal and mutant *Drosophila melanogaster*. *J. Exp. Zool.* **203**, 207–14 (1978).

72. Jia, Q. *et al.* Juvenile hormone and 20-hydroxyecdysone coordinately control the developmental timing of matrix metalloproteinase-induced fat body cell dissociation. *J. Biol. Chem.* **292**, 21504–21516 (2017).

73. Bittova, L. *et al.* Exquisite ligand stereoselectivity of a *Drosophila* juvenile hormone receptor contrasts with its broad agonist repertoire. *J. Biol. Chem.* **294**, 410–423 (2019).

74. Kolonko-Adamska, M. *et al.* Interaction patterns of methoprene-tolerant and germ cell-expressed *Drosophila* JH receptors suggest significant differences in their functioning. *Front. Mol. Biosci.* **10**, 1215550 (2023).

75. Dubrovsky, E. B. *et al.* The *Drosophila* FTZ-F1 nuclear receptor mediates juvenile hormone activation of E75A gene expression through an intracellular pathway. *J. Biol. Chem.* **286**, 33689–700 (2011).

76. Okuda, K. *et al. Leishmania amazonensis* Engages CD36 to Drive Parasitophorous Vacuole Maturation. *PLoS Pathog.* **12**, e1005669 (2016).

77. Shandala, T. *et al. Drosophila* 14-3-3ε has a crucial role in anti-microbial peptide secretion and innate immunity. *J. Cell Sci.* **124**, 2165–74 (2011).

78. Kelly, T. J. *et al.* Juvenile hormone and ovarian maturation in the diptera: A review of recent results. *Insect Biochem.* **17**, 1089–1093 (1987).

79. Soller, M., Bownes, M. & Kubli, E. Control of oocyte maturation in sexually mature *Drosophila* females. *Dev. Biol.* **208**, 337–51 (1999).

80. Dubrovsky, E. B. Hormonal cross talk in insect development. *Trends Endocrinol. Metab.* **16**, 6–11 (2005).

81. Nunes, C., Koyama, T. & Sucena, É. Co-option of immune effectors by the hormonal signaling system triggering metamorphosis in *Drosophila melanogaster*. *PLoS Genet.* **17**, e1009916 (2021).

82. Zhang, Z. & Palli, S. R. Identification of a *cis*-regulatory element required for 20-hydroxyecdysone enhancement of antimicrobial peptide gene expression in *Drosophila melanogaster*. *Insect Mol. Biol.* **18**, 595–605 (2009).

83. Beckstead, R. B., Lam, G. & Thummel, C. S. The genomic response to 20-hydroxyecdysone at the onset of *Drosophila* metamorphosis. *Genome Biol.* **6**, (2005).

84. Meister, M. & Richards, G. Ecdysone and insect immunity: The maturation of the inducibility of the *diptericin* gene in *Drosophila* larvae. *Insect Biochem. Mol. Biol.* **26**, 155–160 (1996).

85. Kang, P. *et al.* NF-κB-mediated developmental delay extends lifespan in *Drosophila*. *Proc. Natl. Acad. Sci. U. S. A.* **122**, e2420811122 (2025).

86. Wang, L. *et al.* Retrotransposon activation during *Drosophila* metamorphosis conditions adult antiviral responses. *Nat. Genet.* **54**, 1933–1945 (2022).

87. Ji, Y. *et al.* The role of 20-hydroxyecdysone and juvenile hormone in insecticidal activity of *Bacillus thuringiensis* regulated by DUOX-ROS immunity in *Spodoptera exigua*. *Pestic. Biochem. Physiol.* **208**, 106222 (2025).

88. Alomar, A. A., Eastmond, B. H. & Alto, B. W. Juvenile hormone analog enhances Zika virus infection in *Aedes aegypti*. *Sci. Rep.* **11**, 21062 (2021).

89. Darby, A. M., Keith, S. A., Kalukin, A. A. & Lazzaro, B. P. Chronic bacterial infections exert metabolic costs in *Drosophila melanogaster*. *Journal of Experimental Biology* **228**, jeb249424 (2025).

90. Hayashi, S. *et al.* GETDB, a database compiling expression patterns and molecular locations of a collection of Gal4 enhancer traps. *Genesis (United States)* **34**, 58–61 (2002).

91. Jenkins, V. K., Larkin, A. & Thurmond, J. Using FlyBase: A Database of *Drosophila* Genes and Genetics. In *Drosophila*: Methods and Protocols, Dahmann C (ed) pp 1–34. New York, NY: Springer US (2022).

92. Giese, C., Spindler, K. D. & Emmerich, H. The Solubility of Insect Juvenile Hormone in Aqueous Solutions and Its Adsorption by Glassware and Plastics. *Z Naturforsch* **32c**, 158-160 (1977).

93. Ramirez, C. E. *et al.* Fast, ultra-trace detection of juvenile hormone III from mosquitoes using mass spectrometry. *Talanta* **159**, 371–378 (2016).

94. McGuire, S. E., Le, P. T., Osborn, A. J., Matsumoto, K. & Davis, R. L. Spatiotemporal Rescue of Memory Dysfunction in *Drosophila*. *Science* **302**, 1765–1768 (2003).

95. Khalil, S., Jacobson, E., Chambers, M. C. & Lazzaro, B. P. Systemic bacterial infection and immune defense phenotypes in *Drosophila melanogaster*. *Journal of Visualized Experiments* **2015**, e52613 (2015).

96. Kassambara A, Kosinski M & Biecek P (2024) survminer: Drawing Survival Curves using ‘ggplot2’. (R package version 0.5.0.999). 2024. Accessed 30 October 2024. https://github.com/kassambara/survminer.

Figure legends

Figure 1. Mating and JH III exposure increases the susceptibility of *D. melanogaster* females to bacterial infection. (A,B) Mated females exhibit higher mortality than unmated females when systemically infected with the bacterium *Providencia rettgeri*. Mated females are more sensitive to infection when challenged either 6 hours **(A)** or 4 days **(B)** after mating. **(C)** Treatment with 1 µg or 2 µg of volatilized, exogenous JH III is sufficient to increase infection susceptibility of unmated females, while lower concentrations do not increase mortality relative to vehicle-exposed control females. **(D)** Unmated females exposed to 2 µg JH III for 24 hours exhibit elevated expression of JH-responsive genes compared to unmated females exposed to acetone vehicle. Bars represent the mean and each point represents an individual replicate, 5-10 females per replicate. Survival data **(A,B,C)** were analyzed by Cox proportional hazards model. Benjamini Hochberg-adjusted, post-hoc pairwise comparisons were used to test for the effect of JH III dose in **(C)**. RT-qPCR data **(D)** were analyzed by unpaired two-sample t-test. Groups with different letters are statistically different from one another ($p<0.05$). n.s.=not significant. Sample sizes are reported in Table S1.

Figure 2. Mating activates a transient peak in JH III titers and sustained JH signaling activity. (A) LC-MS/MS measurements of JH III levels in females over time following mating. JH III levels increase at 2 hours and 6 hours post-mating then decrease and remain consistent from 12 hours through 4 days post-mating. Boxes show median, first and third quartiles, and 1.5x interquartile range. Each point represents an individual replicate of 50 females. **(B)** RT-qPCR analysis of *8xJHRE-eGFP* reporter expression over time following mating. *eGFP* transcript levels, indicative of global JH signaling activity,

increase 6 hours post-mating and remain elevated up to 7 days post-mating relative to age-matched unmated females. Bars represent the mean and each point represents an individual replicate, 5-10 females per replicate. JH III titer data **(A)** were analyzed by Kruskal-Wallis test with Dunn's post hoc comparisons. RT-qPCR data **(B)** were analyzed by unpaired two-sample t-test. Groups with different letters are statistically different from one another while groups sharing letters are not statistically different ($p<0.05$). Sample sizes are reported in Table S1.

Figure 3. Transient activation of JH III signaling is not sufficient to increase infection susceptibility of unmated females. (A) Schematic illustrating experimental design. Unmated females aged 3 days post-eclosion were exposed to 2 µg JH III throughout the experiment with daily transfer to fresh exposure vials ("Repeated exposure" group) or were housed in JH III vials for 48 hours then transferred to regular food vials for the remainder of the experiment ("Transient exposure" group). Transiently exposed females were sampled for LC-MS/MS analysis of JH levels or RT-qPCR analysis of *8xJHRE-eGFP* expression at 6 hours after initiating JH III exposure ("6h"), and 24 hours after JH III removal ("72h-T"), the timepoint at which *P. rettgeri* infections were administered. **(B)** JH III levels in females transiently exposed to the hormone. JH III levels slightly increase 6 hours after exposure and are equivalent to vehicle controls following hormone removal. Boxes show median, first and third quartiles, and 1.5x interquartile range. Each point represents an individual replicate of 50 females. **(C)** RT-qPCR analysis of *8xJHRE-eGFP* reporter expression in transiently exposed females. JH signaling activity increases 6 hours after initial hormone exposure and subsides following hormone removal. Bars represent the mean and each point represents an individual replicate, 5-

10 females per replicate. **(D,E)** Repeated exposure to 2 µg JH III (solid lines) increases *P. rettgeri* infection-induced mortality (as in Fig. 1C), while females transiently exposed to JH III (dashed lines) survive comparably to vehicle-exposed control females. JH III titer data **(B)** were analyzed by Kruskal-Wallis test. RT-qPCR data **(C)** were analyzed by unpaired two-sample t-test. Survival data **(D,E)** were analyzed by Cox proportional hazards model with Benjamini Hochberg-adjusted pairwise comparisons. Groups with different letters are statistically different from one another ($p<0.05$). n.s.=not significant. Sample sizes are reported in Table S1.

Figure 4. The JH receptor Gce is required for mating-induced sensitivity to bacterial infection. (A) Ubiquitous, whole-life RNAi knockdown of *gce* using a GAL4 driver active in the endogenous *gce* expression pattern blocks mating-induced sensitivity to *P. rettgeri* infection. **(B)** Whole-life *gce* RNAi targeted specifically to the fat body prevents mating from increasing female flies' susceptibility to infection. Survival data were analyzed by Cox proportional hazards model with Benjamini Hochberg-adjusted pairwise comparisons. Groups with different letters are statistically different from one another ($p<0.05$). Sample sizes are reported in Table S1.

Figure 5. Mating-induced infection sensitivity requires Gce in the fat body during metamorphosis but not during adulthood. (A) Schematic illustrating timing and duration of developmentally-restricted *gce* knockdown in prior experiments (Fig. 4A, 4B and Schwenke & Lazzaro, 2017) and experiments represented in panels **(B,C,D)**, along with resultant effects on post-mating reduction of infection survival. **(B,C)** Knocking down *gce* in the fat body in the adult stage only **(B)** or beginning at the mid-pupal stage **(C)** does not inhibit mating-induced sensitivity to *P. rettgeri* infection. **(D)** RNAi reduction of

gce expression in the fat body only during metamorphic stages (white prepupae through eclosion) strongly mitigates mating-induced infection susceptibility. Survival data were analyzed by Cox proportional hazards model with Benjamini Hochberg-adjusted pairwise comparisons. Groups with different letters are statistically different from one another ($p<0.05$). Sample sizes are reported in Table S1. “E” = embryo, “WPP” = white prepupae, “P1-P10” = pupal stages 1-10, “PP” = pharate pupae.

Figure 6. Mating-induced infection sensitivity involves Gce in multiple adult tissues. (A) Schematic illustrating the timing of adult-specific activation of *gce* RNAi prior to mating and infection in experiments represented in **(B,C,D)**. **(B)** Knocking down *gce* in the adult brain, fat body, and ovarian follicle cells strongly reduces the increased sensitivity to *P. rettgeri* infection caused by mating. **(C,D)** Adult-specific, ubiquitous *gce* RNAi using either the *gce-T2A-GAL4* driver **(C)** or the *tub-GAL4* driver **(D)** fully eliminates mating-induced susceptibility to *P. rettgeri* infection. Survival data were analyzed by Cox proportional hazards model with Benjamini Hochberg-adjusted pairwise comparisons. Groups with different letters are statistically different from one another ($p<0.05$). Sample sizes are reported in Table S1.

Figure 7. Hypothesized model for JH functions during metamorphosis and post-mating that reduce antibacterial immune defenses of female *D. melanogaster*. Solid arrows indicate effects shown in this study or in prior studies, dashed arrows indicate proposed interactions.

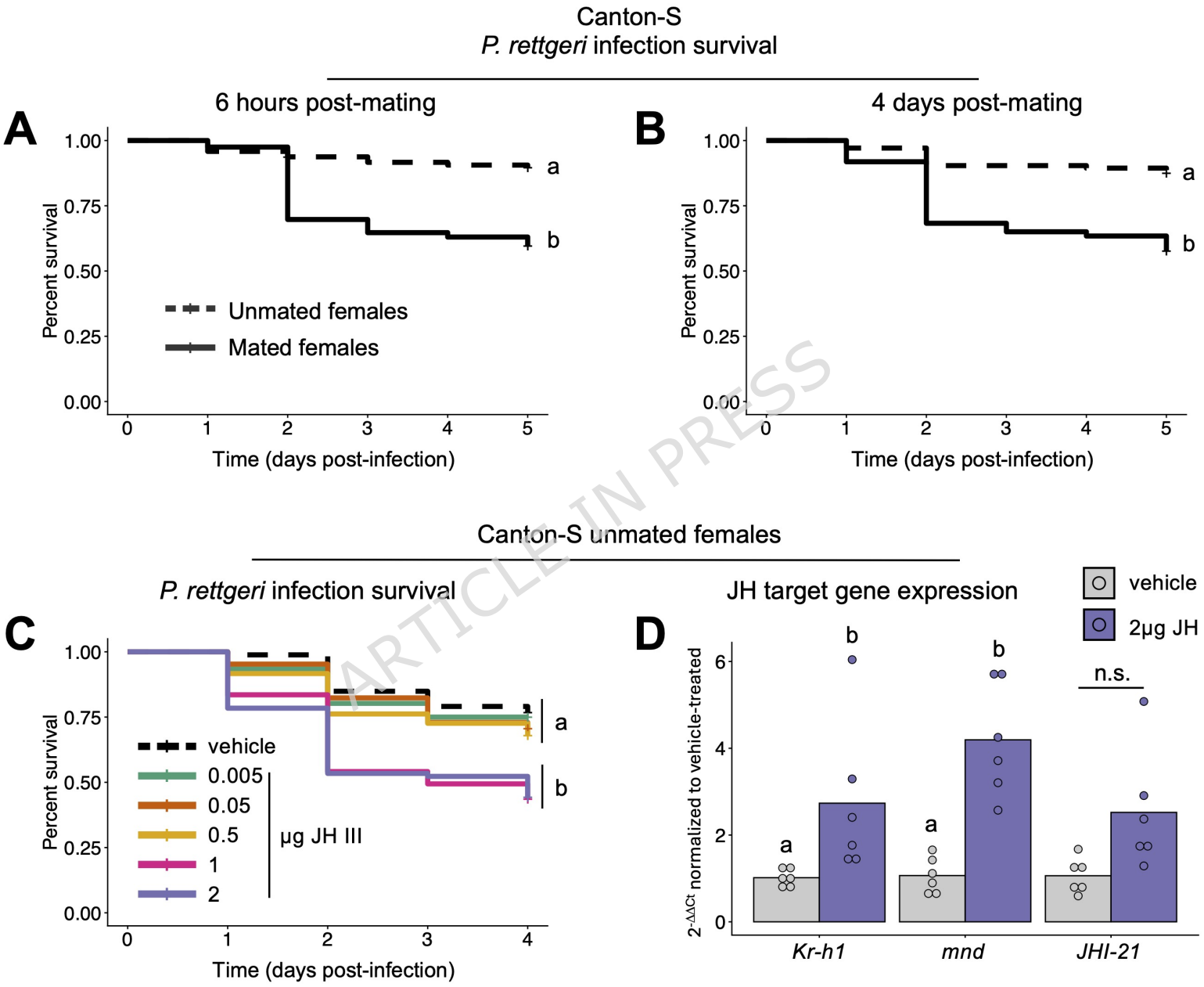

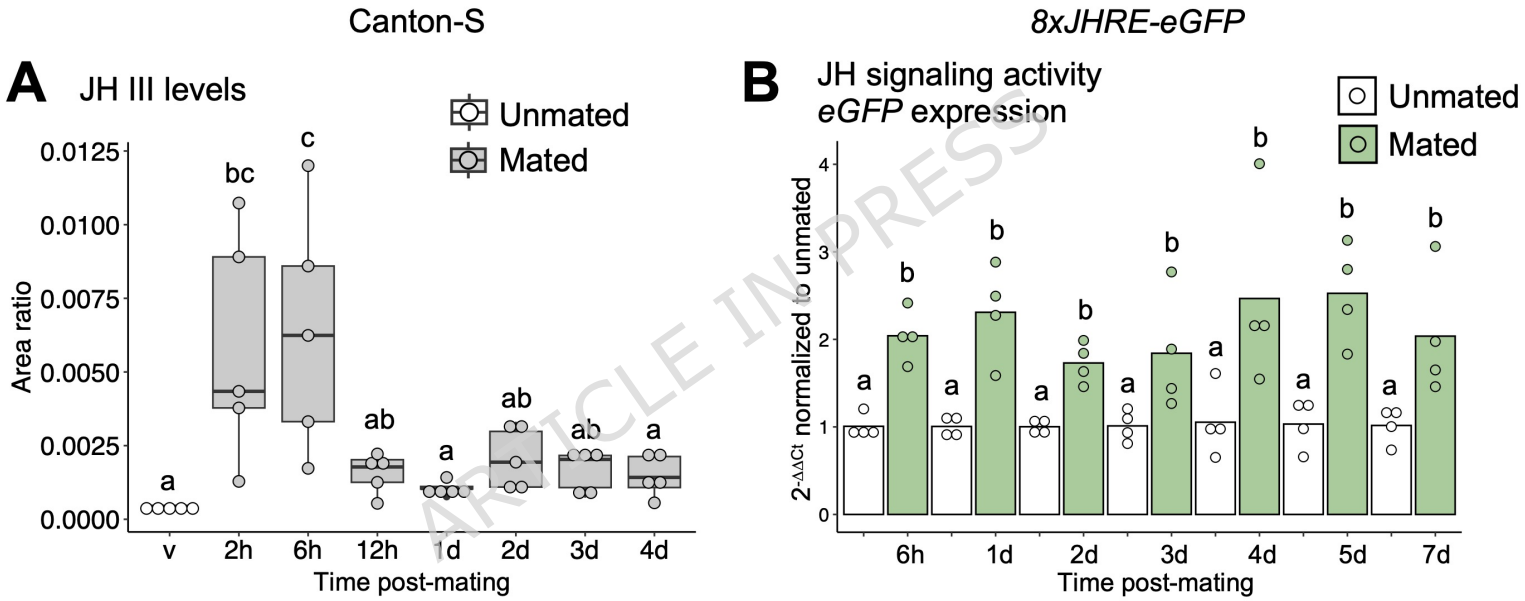

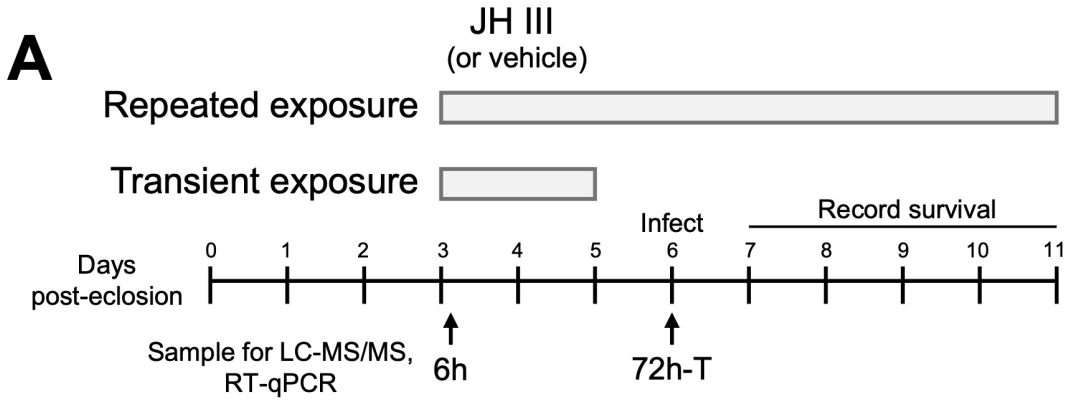

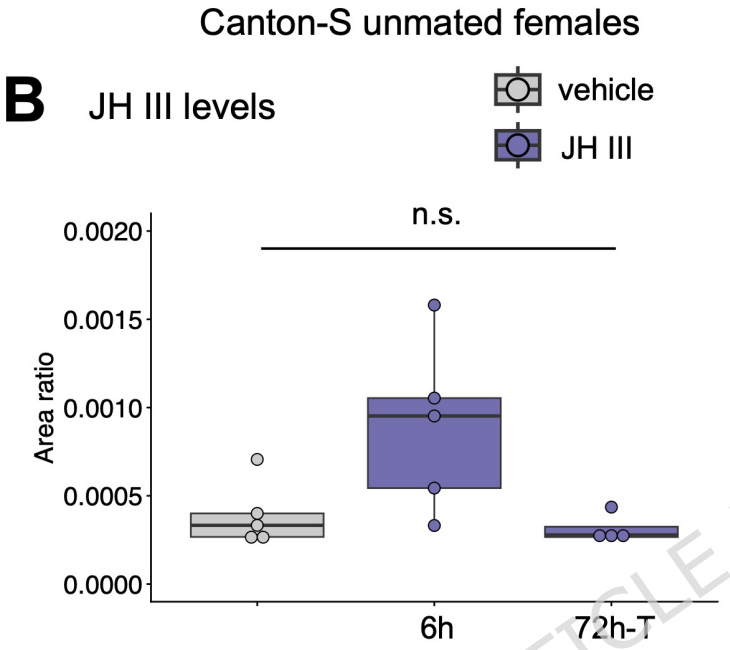

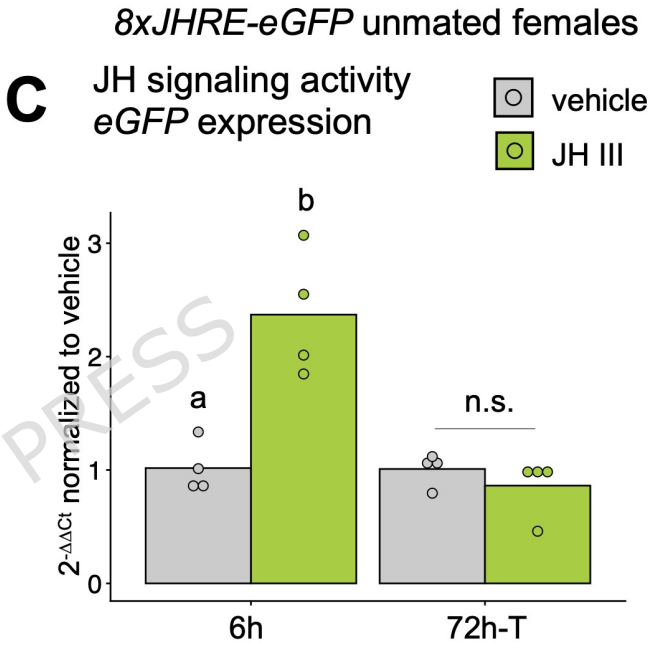

P. rettgeri infection survival